Journal of Basic and Applied Engineering Research
p-ISSN: 2350-0077; e-ISSN: 2350-0255; Volume 3, Issue 12; October-December, 2016, pp. 1064-1067

http://www.krishisanskriti.org/Publication.html

A CFD thermal Performance analysis of Solar Air Heater with Turbulent Promoters

Jitesh Rana[a*], Anshuman Silori[a], Lalit Naagar[a] and Rajesh Maithani[a]

[a]Department of Mechanical Engineering, DIT University, Dehradun (UK)
*E-mail: *jiteshrana95@gmail.com*

Abstract—*Computational fluid dynamics (CFD) analysis of a solar air heater has been carried out using v-rib with symmetrical gaps as artificial roughness on the absorber plate. The relative roughness pitch P/e =10, relative roughness height e/D=0.042, angle of attack α=30°–75° and Reynolds number Re=3000–18,000 are chosen as design variables for analysis. The effect of angle of attack and Reynolds number on the enhancement of Nusselt number and friction factor is also presented*

Nomenclature:

P Pitch of the rib (m)
e/D Relative roughness height
P/e Relative roughness pitch
g/e Relative gap width
Re Reynolds number
e Rib height (m)
η Thermo hydraulic performance parameter
h Convective heat transfer coefficient (W/m^{2}K)
f Friction factor of roughened duct
g Gap size (m)
D Hydraulic diameter of duct (m)
N_g Number of gaps
Nu Nusselt number of roughened duct
Nu_s Nusselt number of smooth duct

1. INTRODUCTION

Solar air heater is one among solar thermal systems which has a wide range of applications such as, space heating, winter home heating, seasoning of timber, drying of crops etc. but the problem with the solar air heater is that they are less efficient. From the study, it was observed that a sub-laminar layer is formed on the absorber plate which further resist the rate of heat transfer between the air and absorber plate and this is the main reason for the poor efficiency of solar air heater. Many of the researchers has performed experimental study [1-3] as well as the CFD analysis on solar air heater with different roughness element to enhance the heat transfer rate. Gupta et al. [4] have carried out a parametric study of artificial roughness geometry in the form of expanded metal mesh type on the absorber plate of solar air heater duct. Saini and Saini [6] by using arc-shaped rib roughness elements attached to the underside of a heated plate reported the experimental prediction of heat transfer characteristics and turbulent fluid flow for a rectangular air channel. The experimental investigation of rectangular duct having its one broad wall heated and roughened with periodic 'discrete V-down rib' was carried out by Singh et al. [7] to study the heat transfer characteristics of solar air heater, and at pitch (P/e) of 8 maximum value of Nusselt number and friction factor was found. A CFD-based analysis of roughened duct with artificial roughness in form of arc-shaped geometry was carried by Kumar and Saini [8] 3-D models was used carry out the heat transfer and flow analysis. FLUENT 6.3.26 commercial CFD code was used for simulation. Different Turbulent Models namely Standard k-ε, Shear stress transport k-u , Realizable k-ε and Renormalization group (RNG) k-ε were tested for smooth duct having the same cross-section of roughened duct in order to find out the validity of the models. An Experimental investigation was carried out by Maithani and Saini [8] with V-ribs with symmetrical gaps ribs on absorber plate of solar air heater duct.

2. CFD FLOW SIMULATION AND MODELING OF RECTANGULAR DUCT

The present work has been carried out using a CFD code ANSYS 15.0.The duct has been made in design modeler. The flow system is a rectangular duct, which is divided into test, entry and exit sections. The 3-d view of the duct with rib attached and the air flow direction is shown in Fig. 1. Different configurations of v-shaped rib roughness used in CFD analysis is given in Table 1.

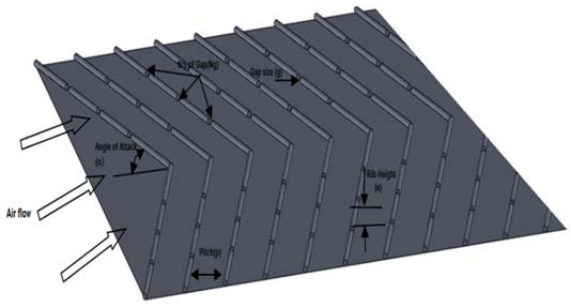

Fig. 1: Computational domain of solar air heater

Table 1: Geometrical parameters of duct used in ANSYS FLUENT 15.0

Geometrical Parameters	values
Length (L)	1100mm
Width (W)	300mm
Height (H)	25mm
Number of gaps (N_g)	4
Gap size (g)	4mm
Angle of attack (α)	30°-75°

3. ANALYSIS

3.1 Grid generation

The complete solution of the fluid flow is the compilation of the results in each cell. In the current analysis non-uniform grid is generated in the computational domain, in the meshing module of ANSYS 15.0 as shown in Fig. 2. The Very fine mesh is used near the boundary of the domain such that the laminar sub-layer can be reduced.

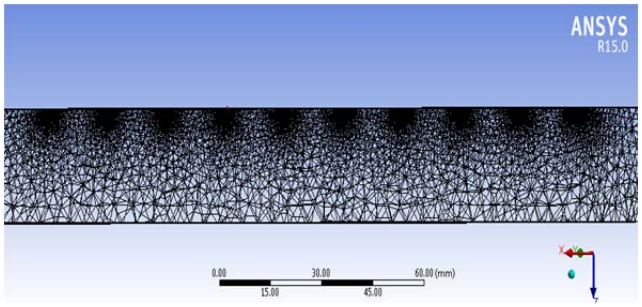

Fig. 2: Non-uniform grid on computational domain

3.2 Mathematical solution in Ansys

The flow equations are solved using RNG k–e turbulence model as it shows very good agreement with the empirical relations. The convergence criteria of 10^{-3} for the residuals of continuity equations, 10^{-6} for the residuals of velocity components and 10^{-6} for the residuals of energy. A CFD code ANSYS 15.0 is used which by using a control volume technique it converts the partial differential governing equations into algebraic equations.

3.3. Validation of CFD model

The CFD results are validated in the form of average Nusselt number and friction factor for a smooth duct with the correlations proposed by Dittus-Boelter and Blasius. Comparison of experimental and predicted values of Nusselt number and friction factor is shown in Fig. 3. The CFD results that are obtained are in good agreement to ensure the accuracy of the data being collected from the experimental investigation.

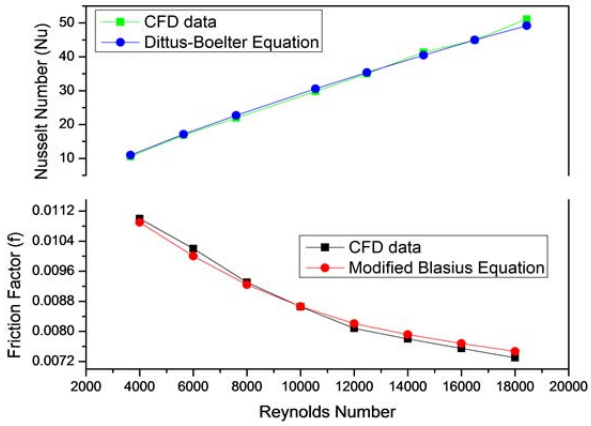

Fig. 3: Comparison of CFD data with Dittuse Boelter empirical correlation and Blasius equation for smooth duct

4. RESULTS AND DISCUSSION

To study the effect of angle of attack (α) on the heat transfer and flow friction characteristics using artificial roughness in the form of v -shaped ribs a CFD analysis of three-dimensional solar air heater duct is carried out

4.1. Turbulence in Kinetic Energy profile

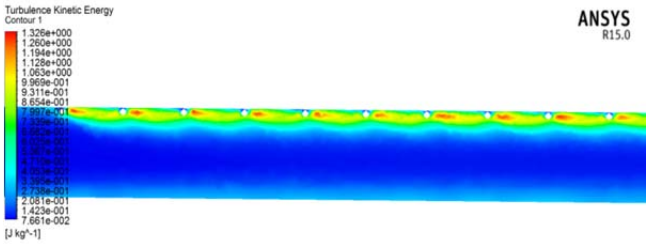

Fig. 4: Contour of turbulence in kinetic energy with angle of attack of 60°

Turbulent kinetic energy is defined as the Mean kinetic energy per unit mass associated with eddies in the Turbulent flow. From the fig 6, it can be seen that between the ribs high turbulence occur which enhances the rate of heat transfer inside the duct.

4.2. Velocity Profile

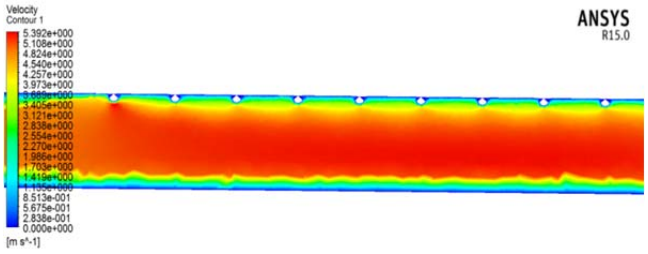

Fig. 5: Contour of velocity profile with angle of attack of 60°

Fig. 5 shows the contour plot of velocity at a fixed value of Reynolds number of 18,000. The plot shows that eddies are generated adjacent to the rib. At high Reynolds number, velocity is high hence disturbances is also high to the laminar sub-layer by the roughness element which minimize the effect of laminar sub layer and as a result enhancement of heat transfer occurs. The contour plots of pressure using CFD analysis for Re = 12,000 and e/D = 0.042 at angle of attack of 60° is shown in Fig. 6

4.3. Pressure Profile

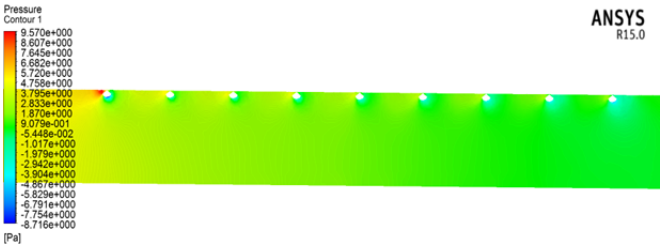

Fig. 6. Contour plots of the pressure angle of attack of 60°.

4.4. Temperature Profile

Fig. 7 shows a 3-D representation of the static temperature in the solar air channel. It can be seen that the fluid temperature Increases throughout the duct, and at the outlet of the solar air channel maximum fluid temperature is found. The ribs are an introduction to break this retarded flow and let it reattach again with the heated surface to enhance the heat transfer. V-ribs produces turbulence by separation and reattachment on the top and the two sides of it.

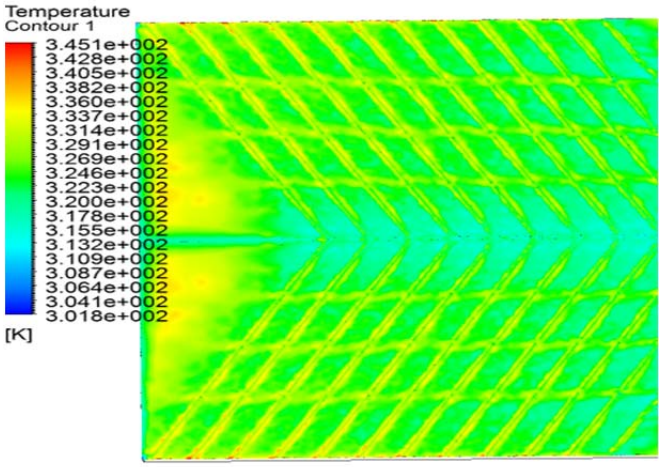

Fig. 7: Contour of temperature profile at Reynolds number 16000

4.5. Flow Pattern

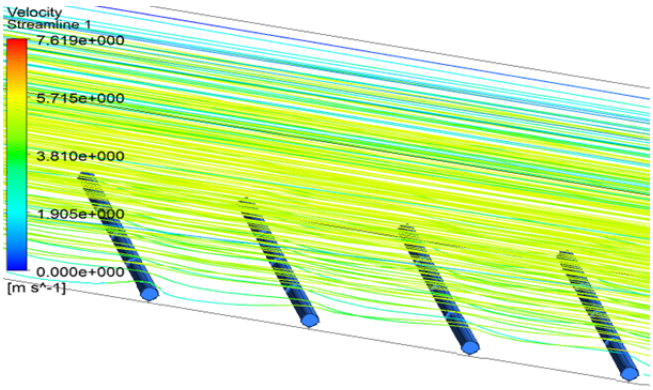

Fig. 8: The attachment and detachment of flow

4.6. Effect of angle of attack (α)

Fig.9. shows a variation of Nusselt number and friction factor with Reynolds number at different values of angle of attack. for the angle of attack of 60° and at Reynolds number 18000 the Nusselt number was found to be maximum, the least value of Nusselt number is obtained for the angle of attack of 30°.The friction factor is also maximum for an angle of attack of 60° and it further decreases with increase in Reynolds number. It was noticed that thermo-hydraulic performance was high for an angle of attack 60° and for an angle of attack 30° thermo-hydraulic performance was found to be low. Fig.10.shows variation of thermo-hydraulic performance with Reynolds number at a different angle of attack. It can also be concluded from the graph that with an increase in Reynolds number thermo-hydraulic performance increases up to 14000 and then starts decreasing.

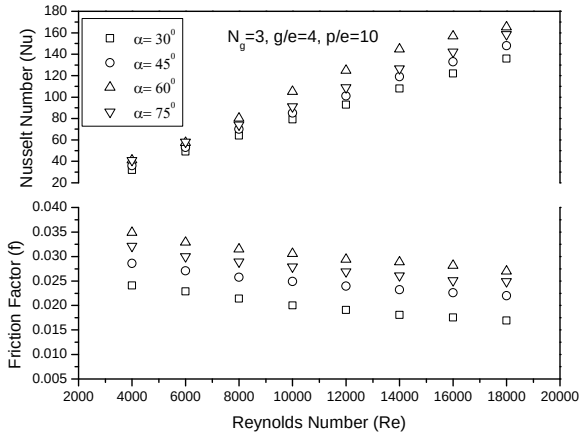

Fig. 9: Variation of Nusselt number and friction factor with Reynolds number at different values of angle of attack

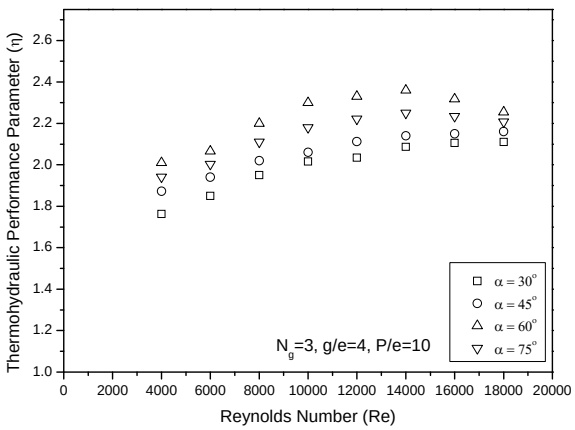

Fig. 10: Shows graph between variations of thermo-hydraulic performance with Reynolds number at different angle of attack

5. CONCLUSION

1. The present study has been done by using Renormalization-group The RNG k–e turbulence model because it predicts very close results to that of experimental results.
2. Average Nusselt number increases with an increase of Reynolds number.
3. Friction factor decreases with increase in Reynolds number, the maximum friction factor is attained at for angle of attack 60°.
4. For an angle of attack 60° thermo-hydraulic performance was found to be high and least for the angle of attack of 30°.
5. Various CFD contours have been shown to visualize the effect of velocity, turbulence in kinetic energy, temperature at different Reynolds number.

REFERENCES

[1] Kumar A, Saini RP, Saini JS. Heat and fluid flow characteristics of roughened solar air heater duct e a review. Renewable Energy 2012;47:77-

[2] A.S. Yadav, J.L. Bhagoria, A CFD-based heat transfer and fluid flow analysis of a solar air heater provided with circular transverse wire rib roughness on the absorber plate, Energy 55 (2013) 1127–1142.

[3] Varun, R.P. Saini, S.K. Singal, Investigation of thermal performance of solar air heater having roughness elements as a combination of inclined and transverse ribs on absorber plate, Renewable Energy 33 (2008) 1398–1405

[4] Gupta MK, Kaushik SC (2009) Performance evaluation of solar air heater having expanded metal mesh as artificial roughness on absorber plate. Int J Thermal Sci 48:1007–1016

[5] Saini, R.P., Saini, J.S., 1997. Heat transfer and friction factor correlations for artificially roughened ducts with expanded metal mesh as roughened element. Int. J. Heat Mass Transfer 40, 973–986

[6] Singh S, Chander S, Saini JS. Heat transfer and friction factor correlations of solar air heater ducts artificially roughened with discrete V-down ribs. Energy 2011; 36:5053e64.

[7] Kumar S, Saini RP. CFD based performance analysis of a solar air heater duct provided with artificial roughness. Renewable Energy 2009; 34:1285-91.

[8] Maithani R., Saini, J.S., "Heat transfer and fluid flow behavior of a rectangular duct roughened with V-ribs with symmetrical gaps", Int. J. Ambient Energy, 2015, DOI: 10.1080/01430750.2015.1100681.